Strongly Correlated Quantum Gas Prepared by Direct Laser Cooling

Pablo Solano,[1] Yiheng Duan,[1] Yu-Ting Chen,[1,2] Alyssa Rudelis,[1] Cheng Chin,[3] and Vladan Vuletić[1,*]
[1]Department of Physics, MIT-Harvard Center for Ultracold Atoms, and Research Laboratory of Electronics, Massachusetts Institute of Technology, Cambridge, Massachusetts 02139, USA
[2]Department of Physics, Harvard University, Cambridge, Massachusetts 02138, USA
[3]James Franck Institute, Enrico Fermi Institute, Department of Physics, University of Chicago, Chicago, Illinois 60637, USA

(Received 12 June 2019; published 24 October 2019)

We create a one-dimensional strongly correlated quantum gas of ^{133}Cs atoms with attractive interactions by direct laser cooling in 300 ms. After compressing and cooling the optically trapped atoms to the vibrational ground state along two tightly confined directions, the emergence of a non-Gaussian time-of-flight distribution along the third, weakly confined direction reveals that the system enters a quantum degenerate regime. We observe a reduction of two- and three-body spatial correlations and infer that the atoms are directly cooled into a highly correlated excited metastable state, known as a super-Tonks-Girardeau gas.

DOI: 10.1103/PhysRevLett.123.173401

Laser trapping and cooling techniques enable the preparation of atomic ensembles at ultracold temperatures, where quantum effects dominate [1,2]. However, exclusively using optical cooling to reach the quantum degenerate regime is challenging: rescattering of cooling light inside an optically dense ensemble causes excess recoil heating [3], while atomic collisions in the presence of light can lead to heating or molecule formation [4]. For these reasons, the standard final step to quantum degeneracy is evaporative cooling [5–9]. However, evaporation is relatively slow, relies on favorable atomic collisional properties, and requires substantial atom loss.

Schemes based on laser cooling alone have recently succeeded in reaching quantum degeneracy [10–12]. Common to those techniques is the reduction of detrimental effects of the cooling light, either by shielding the densest region from the light (for ^{84}Sr) [10] or by using far-off-resonance cooling light (for ^{87}Rb) [11,12] to reduce light-induced collisions. In both cases, the system was in a weakly correlated state with repulsive two-body interactions (scattering length $a > 0$), such that the condensate is stable against collapse.

Among the alkali atoms, ^{133}Cs is notoriously difficult to evaporatively cool. It features large two- and three-body inelastic collision rates [13–15], while its large negative scattering length [13,14,16,17] and associated strong attractive atom-atom interaction result in collapse of a three-dimensional condensate. Condensation of ^{133}Cs was eventually achieved through slow evaporation at low density in a combination of optical and magnetic traps [18] using a magnetic Feshbach resonance to tune the scattering length to a positive value [13,16,17].

A particularly interesting situation arises when the degenerate gas is in a strongly correlated state that cannot be described by a mean-field theory. Such a regime is reached, e.g., when a quantum gas with strong repulsive interactions is so tightly confined in two directions that it becomes effectively one dimensional (1D) [19–24]. Then at sufficiently low linear density, the atoms avoid each other, effectively behaving like fermions in a regime known as a Tonks-Girardeau gas [19,21–23,25–27]. Surprisingly, this behavior persists even at large negative scattering length, in spite of the strong attraction, where the atoms enter a strongly correlated metastable many-body state [28–31]. Such a "super-Tonks-Girardeau" (sTG) gas was previously generated in a pioneering experiment by transferring a Bose-Einstein condensate adiabatically into a two-dimensional (2D) optical lattice [31].

In this Letter, we demonstrate direct laser cooling of a quantum gas with attractive interactions into a strongly correlated sTG state that cannot be described by mean-field theory. The motion along two tightly confined directions x, y is continuously cooled to the quantum ground state by degenerate Raman sideband cooling (dRSC) [32–36]. Along the third, weakly confined z direction, atomic collisions transfer energy to the tightly trapped directions. After compression of the gas of ^{133}Cs atoms into a small array of optical traps and cooling, a non-Gaussian momentum distribution along z emerges, evidencing the onset of quantum degeneracy in this quasi-1D system with large negative scattering length $a = -130$ nm [13,14]. Measurements of inelastic collisions show that spatial two- and three-body correlations are suppressed by almost one and two orders of magnitude, respectively. We infer that the system is directly cooled into a metastable excited gaslike state (sTG gas), stabilized by the strong attractive interaction [28]. Using resonant light for the optical pumping process in dRSC, the sTG gas is prepared in less than 300 ms, more than ten times

faster than previous condensation of ^{133}Cs by evaporative cooling [18,37].

The process begins by loading ^{133}Cs atoms from a magneto-optical trap into a standing-wave trap operating at a wavelength $\lambda = 1064$ nm (x trap, beam waist $w_x = 17$ μm). We then perform dRSC on the 2D gas, optically pumping the atoms into the lowest-energy hyperfine and magnetic sublevel $|F = 3, m = 3\rangle$ of the electronic ground state $^6S_{1/2}$. Trapping light with finely tuned polarization drives Raman transitions transferring atoms to the neighboring magnetic sublevel $|F = 3, m = 2\rangle$ while reducing the vibration quantum number by one. Optical pumping via the $^6P_{3/2}$, $F' = 2$ hyperfine manifold back into $|F = 3, m = 3\rangle$ continuously removes entropy from the system. [See Fig. 1(b) for the atomic level structure and Supplemental Material (SM) [38] for details on trap parameters and cooling procedure.]

After 100 ms of cooling, the 2D gas reaches a temperature of $T = 2.5$ μK and peak classical phase space density (PSD) of PSD ~ 0.1 (see SM [38] for the exact definition). If the cooling were to continue in this geometry, the PSD would subsequently decrease due to light-induced atom loss [4]. We then turn on a second lattice trap (y trap, waist $w_y = 6.5$ μm) transverse to the first one [see Fig. 1(a)]. This configuration creates a 2D array of elongated cigar-shaped traps along the z direction. Immediately after switching on the y trap we adiabatically turn the x trap off and back on to remove atoms not confined to the overlap region of the two traps (see SM for details [38]). This prepares $N \simeq 1000$ atoms distributed in an array of cigar-shaped traps with root mean square size of 1.3×2.5 traps, and a peak occupation of $N_1 \simeq 50$ atoms per trap, as depicted in Fig. 1(c). Because of the spatial compression when turning off the x trap, the atoms' temperature is increased to $T \simeq 5$ μK, at constant PSD [see Fig. 2(a)].

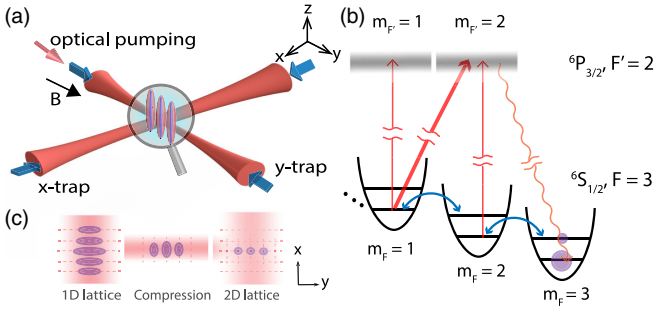

FIG. 1. Experimental setup. (a) Two crossed optical standing waves create a lattice of highly anisotropic cigar-shaped traps. An optical-pumping beam is applied along the y axis, with a magnetic field at a small angle ($\alpha \simeq 10°$) to the y axis. (b) Atomic level structure and cooling procedure. The red arrows represent optical pumping, and the blue arrows represent Raman transitions driven by the trap light. The Raman transition removes one quantum of vibrational energy, while the optical pumping restores the initial internal state. (c) By varying the powers of the two trapping beams in combination with laser cooling, the atoms are compressed into a small number of traps, where a final cooling yields a sTG gas.

The final cooling stage employs two-dimensional dRSC along x and y. The trapping frequencies are $\omega_{x,y} = 2\pi \times 50$ kHz in the transverse directions and $\omega_z = 2\pi \times 2.9$ kHz along the weakly confined direction. After 120 ms of cooling, the 2D ground state in the xy plane is reached [see Fig. 2(b)]. We determine the gas temperature $T_{x,y}$ in the transverse direction by measuring the excess kinetic energy over the harmonic oscillator zero point energy, obtaining $T_{x,y} = (0.2 \pm 0.2)$ μK. For our experimental parameters and observed kinetic energy K_z along the z direction, the corresponding temperature T_z is still close to its classical value $T_z = 2K_z/k_B$ [40,41], yielding $T_z \approx (1.2 \pm 0.1)$ μK. The cooling limit along z is likely set by the collisional thermalization rate between the directly cooled xy directions and the z direction. This rate is exponentially suppressed at $k_B T_{x,y} \ll \hbar\omega_{xy}$ [42,43], and we estimate a minimum possible temperature of $T_z \sim 0.8$ μK for our

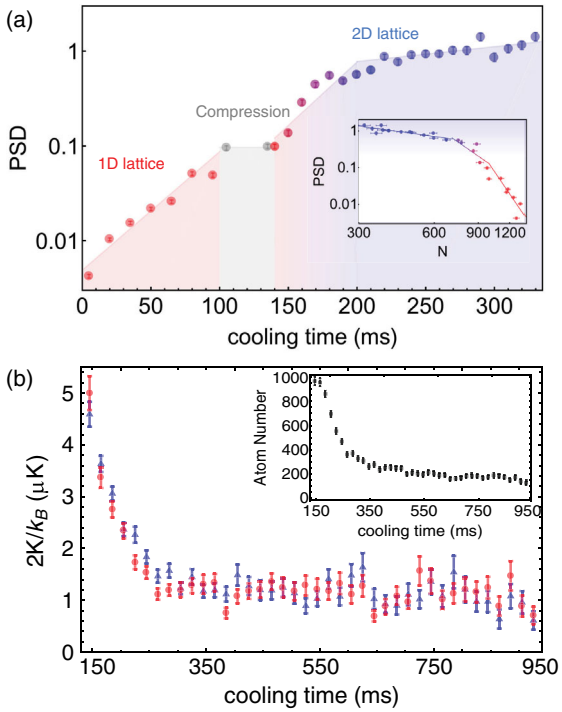

FIG. 2. (a) Phase space density during the cooling sequence. Following a precooling stage (red region), the atoms are compressed in 40 ms into fewer traps (see text). During the final cooling stage the system crosses over into a quantum degenerate region. The inset shows the efficiency of the cooling, displaying the PSD against the remaining atom number. The blue shaded region in the inset represents the PSD at which quantum degeneracy becomes observable. (b) Kinetic energies K_z (red dots) and K_{xy} (blue triangles) of the atoms after sudden release from the trap in a time-of-flight measurement, as a function of cooling time. The inset shows the atom number as a function of cooling time.

parameters (see SM [38]). The higher observed T_z could be explained by some residual heating in the z direction.

During cooling, atoms are lost at a moderate rate due to light-assisted inelastic collisions; once the atoms are cooled to the 2D ground state, the loss rate is substantially reduced, presumably due to the lower cooling and associated photon scattering rate. The two-body loss acts to equalize the populations in different traps, and after 200 ms of two-dimensional dRSC we have 50 mostly equally filled traps with $N_1 = 6 \pm 2$ atoms in each, for a total atom number $N \simeq 300 \pm 100$. (Here the dominant uncertainty is the systematic uncertainty in total atom number, see SM [38].) The local peak density is $n_0 = 1.1 \times 10^{15}$ cm^{-3}.

The evolution of the classical PSD throughout the cooling sequence is shown in Fig. 2(a). The cooling efficiency in the presence of atom loss can be characterized by the logarithmic slope of PSD increase to atom number loss, $\eta = -[d(\ln \mathrm{PSD})/d(\ln N)]$. During the precooling stage, up to PSD ~ 0.5, we observe a very high efficiency $\eta = 10 \pm 0.3$ [see inset of Fig. 2(a)], whereas a typical evaporative cooling has $\eta \sim 3$–4, with the highest reported values $\eta \simeq 6$ [37,44]. For values PSD $\gtrsim 0.5$, the classical PSD no longer coincides with the (higher) occupation per quantum state, and should only be regarded as a qualitative measure of cooling efficiency.

During the final cooling stage [Fig. 2(b)], the momentum distribution observed in a time-of-flight (TOF) measurement remains Gaussian in the tightly confined direction, while a non-Gaussian momentum distribution emerges along the z direction (Fig. 3). The observed z momentum distribution qualitatively agrees with theoretical simulations of a one-dimensional trapped gas of hard-core bosons at similar temperatures in the quantum degenerate regime [41,45]. We employ a bimodal fit to characterize the degree of quantum degeneracy by the ratio N_0/N of the area N_0 under a central peak and the total area under the TOF curve N (see SM for details [38]). We observe a maximum ratio $N_0/N \simeq 0.37$ after 400 ms of cooling [see Fig. 3(d)]. 1D systems exhibit a smooth crossover to quantum-degeneracy [46,47], and we observe a small quantum degenerate component even for PSD < 1.

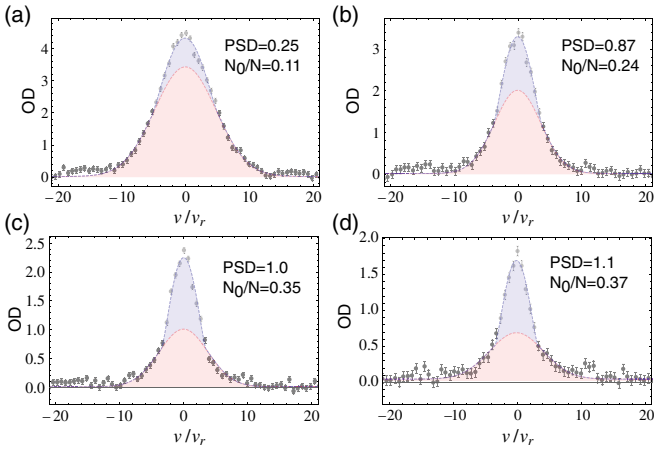

FIG. 3. Velocity distribution of the atoms after sudden release from the trap, normalized by the recoil velocity ($v_r = 3.5$ mm/s). Each plot is an average of 800 TOF images. (a)–(d) Momentum distribution along the direction of weak confinement after 20, 100, 200, and 400 ms of cooling, respectively. The red area represents the fit of a Gaussian distribution to the wings, and the blue area represents the fit of the data minus the Gaussian distribution to a parabola. The value of N_0/N is determined from the ratio of the blue over the total area. (d) Reduced χ^2 of the fit to a single Gaussian is $\chi^2 > 12$, while for the bimodal distribution it is $\chi^2 = 1.17$.

The cooling prepares the system in a strongly correlated, effectively 1D state that survives at large negative scattering length and high density, and is largely immune to two-body radiative losses and three-body recombination loss. Effectively 1D systems can be characterized by the combination of linear density n_{1D} and 1D scattering length, given by $a_{1D} = -a_\perp[(a_\perp/a) - C]$, where $a_\perp = \sqrt{\hbar/m\omega_{x,y}}$ is the ground-state size in the transverse directions, m the atomic mass, a the three-dimensional scattering length, and $C \approx 1.0326$ a constant [25]. The strength of the interactions is characterized by the dimensionless parameter $\gamma = 2/(n_{1D}|a_{1D}|)$ that can be interpreted as the ratio of interaction energy to kinetic energy [22,23]. $\gamma \ll 1$ corresponds to a weakly interacting Bose gas, while $\gamma \gg 1$ describes a strongly interacting Tonks-Girardeau gas (sTG gas) for $a_{1D} < 0$ ($a_{1D} > 0$).

For our parameters with three-dimensional scattering length $a = -130$ nm and $|a| > a_\perp = 39$ nm, the system is in the unitary regime with $a_\perp \approx a_{1D} = 52$ nm. According to Ref. [41], the spatial in-trap distribution along z at our temperatures is still well approximated by a thermal Gaussian distribution. Then the local density approximation yields a value $\gamma_0 = 8 \pm 3$ at the trap center, with the uncertainty being dominated by that of the atom number N_1. An sTG gas has been predicted to be stable against attraction-induced collapse for $\gamma > \gamma_c = 5.7$ [28], and we observed a lifetime exceeding several hundred ms. The near-coincidence $\gamma_0 \approx \gamma_c$ may indicate that the number of atoms in our traps is limited by the stability condition of the sTG gas.

Similar to the Tonks-Girardeau gas, the sTG gas is a highly correlated state where the spatial wave function of the bosons is "fermionized." The associated suppression of two- and three-body short-range correlations $g^{(2)}$ and $g^{(3)}$ has been previously observed for the Tonks gas with repulsive interactions [21,48], but not for the sTG gas. In the following, we investigate experimentally this suppression $g^{(2)}$, $g^{(3)} < 1$ that is expected to persist even at finite temperature [28,30].

The two-body short-range atom-atom correlation function $g^{(2)}$ can be probed with light-assisted loss [49]. The loss rate constant Γ with $\dot{N} = -\Gamma N$, is given by $\Gamma = Gg^{(2)}\langle n \rangle$, where G is the light-induced loss rate constant

set by the light intensity and detuning, and $\langle n \rangle$ is the average atomic density. While G is difficult to evaluate from first principles, we can keep the laser power and detuning constant while changing the dimensionality of our system. To this end, we reduce the x confinement by a variable factor after quantum degeneracy in the cigar-shaped traps has been reached. Figure 4(a) shows the observed ratio $\Gamma/\langle n \rangle = G g^{(2)}$ as a function of vibration frequency ratio ω_x/ω_y. The loss rate constant Γ is measured, and $\langle n \rangle$ is calculated from the measured average kinetic energy, atom number N, and trap vibration frequencies. Compared to a 2D gas ($\omega_x/\omega_y = 0$), the density-normalized light-induced loss rate Γ/n is substantially reduced for the 1D gas ($\omega_x/\omega_y = 1$) by a factor 20. Part of that change can be attributed to the change of G with dimensionality: Pairs of atoms are excited by the light near the Condon point r_C in interatomic distance [4], which for resonant light of wavelength λ is at $r_C \sim \lambda/(2\pi)$, while the atoms are confined to a smaller distance scale $a_\perp$ in the direction of tight confinement. Consequently we expect a reduced loss rate constant G_{1D} compared to G_{2D} by a factor $G_{1D}/G_{2D} \approx a_\perp/r_C = 0.3$ (see SM). Taking this into account, we find from our measurements $g^{(2)}_{2D}/g^{(2)}_{1D} \approx 5$, i.e., $g^{(2)}_{1D} \approx 0.4 \pm 0.2$. While the fractional error in $g^{(2)}_{1D}$ is large due to model-dependent uncertainties for the light-induced loss (see SM [38]), our measurement nonetheless demonstrates suppression of two-body correlations of the same order as the theoretically expected value $g^{(2)}_{1D} = 0.4$ for an sTG gas with $\gamma = 8$ [30].

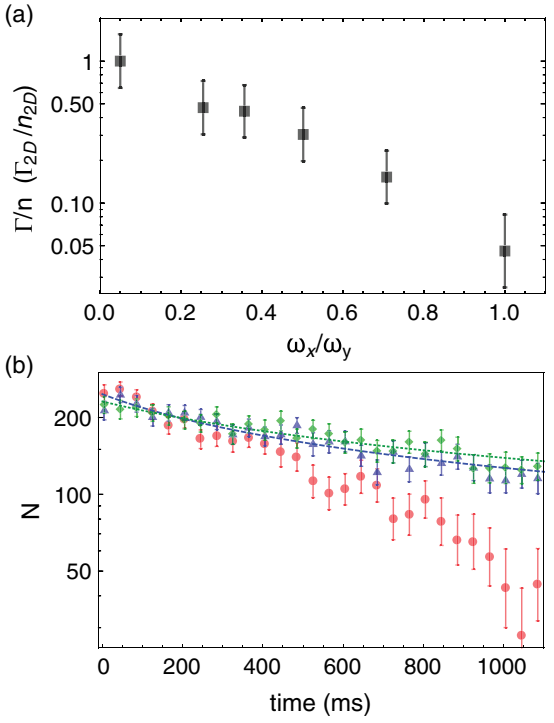

FIG. 4. (a) Density-normalized two-body loss rate as a function of the dimensionality of the gas in the presence of cooling light. ω_x is being varied at fixed $\omega_y/(2\pi) = 50$ kHz between $\omega_x/\omega_y = 0$ and $\omega_x/\omega_y = 1$. The kinetic energy K_z is constant at $2K_z/k_B = 1.2$ μK. (b) Three-body loss in the absence of cooling light for a 2D gas (green diamonds, $\omega_x/\omega_y = 0$), a 1D gas (blue triangles, $\omega_x/\omega_y = 1$), and in between (red circles, $\omega_x/\omega_y = 0.25$). The dotted lines are fits to three-body loss, and the initial kinetic energy the same as in (a). For the 1D gas, the density is 13 times higher than for the 2D gas, while the three-body loss rate is only increased by a factor of 1.4. The atom number evolution in the intermediate regime between 1D and 2D, $\omega_x/\omega_y = 0.25$, cannot be described by three-body loss.

Three-body correlations $g^{(3)}$ can be measured by turning off the cooling light after reaching the quantum degenerate regime, and observing the atom number evolution as a function of dimensionality between $\omega_x/\omega_y = 0$ (2D gas) and $\omega_x/\omega_y = 1$ (1D gas). We measure the atom loss vs time and fit the data to the functional form for three-body loss (see Fig. 4, and SM [38] for details). Comparing the 2D and 1D gases, we observe a suppression of three-body recombination rate constant by a factor of 120 ± 30. [$K_{1D} = (4 \pm 2) \times 10^{-28}$ cm^6 s^{-1} and $K_{2D} = (5 \pm 3) \times 10^{-26}$ cm^6 s^{-1} for the 1D gas and 2D gas, respectively. The 2D case is in agreement with theoretical predictions for a 3D gas [50]]. This provides strong evidence that the 1D nature of the system is protecting the dense gas from three-body loss. The measured value $g^{(3)}_{1D} \approx 0.05 \pm 0.03$ is in agreement with the theoretically expected value for our interaction parameter γ and temperature of $g^{(3)}_{1D} \approx 0.06$ [30]. The dominant uncertainty in $g^{(3)}_{1D}$ arises from the systematic uncertainty in atom number per trap N_1.

Both for the 1D and the 2D gas we observe a time dependence that is well fitted by three-body decay [Fig. 4(b)]. Surprisingly, for an intermediate regime between 1D and 2D (red circles), the atom loss does not follow the characteristic behavior of three-body loss, but the loss speeds up at late times, and very few atoms survive. We hypothesize that the rapid atom loss is due to collapse of the gas at high atomic density in the 1D-2D crossover region when the dimensionality of the system no longer protects the gas against attraction-induced collapse.

In conclusion, we have demonstrated direct laser cooling into a strongly interacting metastable excited phase, an sTG gas. The method is fast and robust, preparing a strongly correlated quantum gas in 300 ms, and enabling measurements with high signal-to-noise ratio. In the future, it will be interesting to tune the scattering length by means of a Feshbach resonance [13,14,16,17], and expand previous studies of Tonks-Girardeau [22,23] and sTG [31] gases with improved signal-to-noise ratio. The demonstrated scheme presents a promising tool for reaching quantum degeneracy in atoms with unfavorable collision properties, and can potentially be extended to optically trapped molecules [51].

This work was supported by the NSF, the NSF Center for Ultracold Atoms, MURI grants through AFOSR and ARO, and NASA. C. C. acknowledges support from NSF Grant No. PHY-1511696, and the University of Chicago MRSEC, funded by the NSF under Grant No. DMR-1420709. We are grateful to F. Salces-Carcoba, Alban Urvoy, Zachary Vendeiro, and Martin Zwierlein for stimulating discussions.

*Corresponding author.
vuletic@mit.edu

[1] W. D. Phillips, Rev. Mod. Phys. **70**, 721 (1998).
[2] J. Dalibard and C. Cohen-Tannoudji, J. Opt. Soc. Am. B **6**, 2023 (1989).
[3] Y. Castin, J. I. Cirac, and M. Lewenstein, Phys. Rev. Lett. **80**, 5305 (1998).
[4] K. Burnett, P. S. Julienne, and K.-A. Suominen, Phys. Rev. Lett. **77**, 1416 (1996).
[5] K. B. Davis, M. O. Mewes, M. R. Andrews, N. J. van Druten, D. S. Durfee, D. M. Kurn, and W. Ketterle, Phys. Rev. Lett. **75**, 3969 (1995).
[6] M. H. Anderson, J. R. Ensher, M. R. Matthews, C. E. Wieman, and E. A. Cornell, Science **269**, 198 (1995).
[7] C. C. Bradley, C. A. Sackett, J. J. Tollett, and R. G. Hulet, Phys. Rev. Lett. **75**, 1687 (1995).
[8] B. DeMarco and D. S. Jin, Science **285**, 1703 (1999).
[9] M. Lu, N. Q. Burdick, S. H. Youn, and B. L. Lev, Phys. Rev. Lett. **107**, 190401 (2011).
[10] S. Stellmer, B. Pasquiou, R. Grimm, and F. Schreck, Phys. Rev. Lett. **110**, 263003 (2013).
[11] J. Hu, A. Urvoy, Z. Vendeiro, V. Crépel, W. Chen, and V. Vuletić, Science **358**, 1078 (2017).
[12] A. Urvoy, Z. Vendeiro, J. Ramette, A. Adiyatullin, and V. Vuletić, Phys. Rev. Lett. **122**, 203202 (2019).
[13] P. J. Leo, C. J. Williams, and P. S. Julienne, Phys. Rev. Lett. **85**, 2721 (2000).
[14] C. Chin, V. Vuletić, A. J. Kerman, and S. Chu, Phys. Rev. Lett. **85**, 2717 (2000).
[15] T. Kraemer, M. Mark, P. Waldburger, J. G. Danzl, C. Chin, B. Engeser, A. D. Lange, K. Pilch, A. Jaakkola, H.-C. Nägerl, and R. Grimm, Nature (London) **440**, 315 (2006).
[16] V. Vuletić, C. Chin, A. J. Kerman, and S. Chu, Phys. Rev. Lett. **83**, 943 (1999).
[17] C. Chin, R. Grimm, P. Julienne, and E. Tiesinga, Rev. Mod. Phys. **82**, 1225 (2010).
[18] T. Weber, J. Herbig, M. Mark, H.-C. Nägerl, and R. Grimm, Science **299**, 232 (2003).
[19] H. Moritz, T. Stöferle, M. Köhl, and T. Esslinger, Phys. Rev. Lett. **91**, 250402 (2003).
[20] T. Stöferle, H. Moritz, C. Schori, M. Köhl, and T. Esslinger, Phys. Rev. Lett. **92**, 130403 (2004).
[21] B. Laburthe Tolra, K. M. O'Hara, J. H. Huckans, W. D. Phillips, S. L. Rolston, and J. V. Porto, Phys. Rev. Lett. **92**, 190401 (2004).
[22] T. Kinoshita, T. Wenger, and D. S. Weiss, Science **305**, 1125 (2004).
[23] B. Paredes, A. Widera, V. Murg, O. Mandel, S. Fölling, I. Cirac, G. V. Shlyapnikov, T. W. Hänsch, and I. Bloch, Nature (London) **429**, 277 (2004).
[24] L. A. Zundel, J. M. Wilson, N. Malvania, L. Xia, J.-F. Riou, and D. S. Weiss, Phys. Rev. Lett. **122**, 013402 (2019).
[25] M. Olshanii, Phys. Rev. Lett. **81**, 938 (1998).
[26] V. Dunjko, V. Lorent, and M. Olshanii, Phys. Rev. Lett. **86**, 5413 (2001).
[27] J. M. Wilson, N. Malvania, Y. Le, Y. Zhang, M. Rigol, and D. S. Weiss, arXiv:1908.05364.
[28] G. E. Astrakharchik, D. Blume, S. Giorgini, and B. E. Granger, Phys. Rev. Lett. **92**, 030402 (2004).
[29] G. E. Astrakharchik, J. Boronat, J. Casulleras, and S. Giorgini, Phys. Rev. Lett. **95**, 190407 (2005).
[30] M. Kormos, G. Mussardo, and A. Trombettoni, Phys. Rev. A **83**, 013617 (2011).
[31] E. Haller, M. Gustavsson, M. J. Mark, J. G. Danzl, R. Hart, G. Pupillo, and H.-C. Nägerl, Science **325**, 1224 (2009).
[32] V. Vuletić, C. Chin, A. J. Kerman, and S. Chu, Phys. Rev. Lett. **81**, 5768 (1998).
[33] S. E. Hamann, D. L. Haycock, G. Klose, P. H. Pax, I. H. Deutsch, and P. S. Jessen, Phys. Rev. Lett. **80**, 4149 (1998).
[34] A. J. Kerman, V. Vuletić, C. Chin, and S. Chu, Phys. Rev. Lett. **84**, 439 (2000).
[35] D.-J. Han, S. Wolf, S. Oliver, C. McCormick, M. T. DePue, and D. S. Weiss, Phys. Rev. Lett. **85**, 724 (2000).
[36] I. Bouchoule, M. Morinaga, C. Salomon, and D. S. Petrov, Phys. Rev. A **65**, 033402 (2002).
[37] C.-L. Hung, X. Zhang, N. Gemelke, and C. Chin, Phys. Rev. A **78**, 011604(R) (2008).
[38] See Supplemental Material at http://link.aps.org/supplemental/10.1103/PhysRevLett.123.173401 for details on the dipole trap loading, which includes Ref. [39].
[39] K. Shibata, S. Yonekawa, and S. Tojo, Phys. Rev. A **96**, 013402 (2017).
[40] M. J. Davis, P. B. Blakie, A. H. van Amerongen, N. J. van Druten, and K. V. Kheruntsyan, Phys. Rev. A **85**, 031604(R) (2012).
[41] Y. Hao, Y. Song, and X. Fu, Int. J. Mod. Phys. B **30**, 1650216 (2016).
[42] D. S. Petrov and G. V. Shlyapnikov, Phys. Rev. A **64**, 012706 (2001).
[43] I. E. Mazets and J. Schmiedmayer, New J. Phys. **12**, 055023 (2010).
[44] A. J. Olson, R. J. Niffenegger, and Y. P. Chen, Phys. Rev. A **87**, 053613 (2013).
[45] G. J. Lapeyre, M. D. Girardeau, and E. M. Wright, Phys. Rev. A **66**, 023606 (2002).
[46] D. S. Petrov, G. V. Shlyapnikov, and J. T. M. Walraven, Phys. Rev. Lett. **85**, 3745 (2000).
[47] I. Bouchoule, K. V. Kheruntsyan, and G. V. Shlyapnikov, Phys. Rev. A **75**, 031606(R) (2007).
[48] E. Haller, M. Rabie, M. J. Mark, J. G. Danzl, R. Hart, K. Lauber, G. Pupillo, and H.-C. Nägerl, Phys. Rev. Lett. **107**, 230404 (2011).
[49] T. Kinoshita, T. Wenger, and D. S. Weiss, Phys. Rev. Lett. **95**, 190406 (2005).
[50] U. Eismann, L. Khaykovich, S. Laurent, I. Ferrier-Barbut, B. S. Rem, A. T. Grier, M. Delehaye, F. Chevy, C. Salomon, L.-C. Ha, and C. Chin, Phys. Rev. X **6**, 021025 (2016).
[51] L. Anderegg, B. L. Augenbraun, Y. Bao, S. Burchesky, L. W. Cheuk, W. Ketterle, and J. M. Doyle, Nat. Phys. **14**, 890 (2018).